



LAWRENCE
LIVERMORE
NATIONAL
LABORATORY

Late Holocene Radiocarbon Variability in Northwest Atlantic Slope Waters

O. Sherwood, E. Edinger, T. P. Guilderson, B.
Ghaleb, M. J. Risk, D. B. Scott

August 20, 2008

Earth and Planetary Science Letters

Disclaimer

This document was prepared as an account of work sponsored by an agency of the United States government. Neither the United States government nor Lawrence Livermore National Security, LLC, nor any of their employees makes any warranty, expressed or implied, or assumes any legal liability or responsibility for the accuracy, completeness, or usefulness of any information, apparatus, product, or process disclosed, or represents that its use would not infringe privately owned rights. Reference herein to any specific commercial product, process, or service by trade name, trademark, manufacturer, or otherwise does not necessarily constitute or imply its endorsement, recommendation, or favoring by the United States government or Lawrence Livermore National Security, LLC. The views and opinions of authors expressed herein do not necessarily state or reflect those of the United States government or Lawrence Livermore National Security, LLC, and shall not be used for advertising or product endorsement purposes.

Late Holocene Radiocarbon Variability in Northwest Atlantic Slope Waters

Owen A. Sherwood ^{1*}, Evan N. Edinger ², Thomas P. Guilderson ^{3,4}, Bassam Ghaleb ⁵,
Michael J. Risk ⁶, David B. Scott ⁷

¹ Department of Biology, Memorial University of Newfoundland, St. John's NL, Canada,
A1B 3X9.

² Departments of Biology and Geography, Memorial University of Newfoundland,
St. John's NL, Canada, A1B 3X9.

³ Center for Accelerator Mass Spectrometry, Lawrence Livermore National Laboratory,
Livermore, CA, USA, 94551.

⁴ Department of Ocean Sciences & Institute of Marine Sciences, University of California
Santa Cruz, Santa Cruz, CA, USA, 95064

⁵ Centre GEOTOP-UQAM-McGill, CP 8888, Succ. Centre-Ville, Montreal, QC, Canada,
H3C 3P8

⁶ School of Geography and Geology, McMaster University, Hamilton, ON, Canada,
L8S 4M1

⁷ Centre for Environmental and Marine Geology, Dalhousie University, Halifax, NS,
Canada, B3H 4J1

* Corresponding author
Email: osherwood@gmail.com
Tel: 709-737-8025

Revised for *Earth and Planetary Science Letters*, August 13, 2008

Abstract

Deep-sea gorgonian corals secrete a 2-part skeleton of calcite, derived from dissolved inorganic carbon at depth, and gorgonin, derived from recently fixed and exported particulate organic matter. Radiocarbon contents of the calcite and gorgonin provide direct measures of seawater radiocarbon at depth and in the overlying surface waters, respectively. Using specimens collected from Northwest Atlantic slope waters, we generated radiocarbon records for surface and upper intermediate water layers spanning the pre- and post bomb- ^{14}C eras. In Labrador Slope Water (LSW), convective mixing homogenizes the pre-bomb $\Delta^{14}\text{C}$ signature ($-67 \pm 4 \text{ ‰}$) to at least 1000 m depth. Surface water bomb- ^{14}C signals were lagged and damped (peaking at $\sim +45 \text{ ‰}$ in the early 1980s) relative to other regions of the northwest Atlantic, and intermediate water signals were damped further. Off southwest Nova Scotia, the vertical gradient in $\Delta^{14}\text{C}$ is much stronger. In surface water, pre-bomb $\Delta^{14}\text{C}$ averaged $-75 \pm 5 \text{ ‰}$. At 250-475 m depth, pre-bomb $\Delta^{14}\text{C}$ oscillated quasi-decadally between -80 and -100 ‰ , likely reflecting interannual variability in the presence of Labrador Slope Water vs. Warm Slope Water (WSW). Finally, subfossil corals reveal no systematic changes in vertical $\Delta^{14}\text{C}$ gradients over the last 1200 years.

Key words: radiocarbon, bomb- ^{14}C , vertical gradient, deep-sea corals, Northwest Atlantic

1. Introduction

The radiocarbon content of dissolved inorganic carbon (DIC) in seawater is an important tracer of oceanic mixing. Radiocarbon produced naturally in the atmosphere is taken up in surface waters and mixed downward into deep waters where it undergoes radioactive decay. Uptake of bomb- ^{14}C produced by atmospheric nuclear weapons testing in the late 1950s and early 1960s has amplified the natural ^{14}C gradient between surface and deep waters. While radiocarbon distribution in the world oceans was mapped during the Geochemical Ocean Sections (GEOSECS; Östlund et al., 1987) and subsequent Transient Tracers in the Ocean (TTO) and World Ocean Circulation Experiment (WOCE; Key et al., 2004) expeditions, spatial and temporal variability in seawater ^{14}C is better revealed through study of biogenic archives, such as corals, whose skeletal ^{14}C contents closely reflect that of the seawater in which they grow (Druffel, 1980; Guilderson et al., 1998). Proxy ^{14}C records are useful for constraining marine reservoir ages (Ingram and Southon, 1996; Bondevik et al., 1999; Guilderson et al., 2005), vertical and lateral mixing (Druffel, 1997; Guilderson et al., 2004; Robinson et al., 2005) and air-sea CO_2 exchange (Broecker et al., 1985; Cember, 1989; Fallon et al., 2003). Bomb- ^{14}C records are also useful for establishing or validating skeletal chronologies in a variety of organisms (Campana et al., 2002; Kerr et al., 2005; Roark et al., 2006; Kilada et al., 2007).

Deep-sea corals present new archives of seawater ^{14}C , particularly in high-latitude and deep-water environments, where proxy archives generally are scarce (Adkins et al., 1998, 2002; Mangini et al., 1998). Previous work has focused on aragonitic scleractinian species, which are relatively easily dated with U/Th techniques (Cheng et al., 2000;

Goldstein et al., 2001; Schröder-Ritzrau et al., 2003; Frank et al., 2004; Robinson et al., 2005; Eltgroth et al., 2006; Cao et al., 2007; Sikes et al., 2008). Deep-sea gorgonian corals secrete a 2-part skeleton of calcite and proteinaceous gorgonin. The calcite is derived from dissolved inorganic carbon at depth, while the gorgonin is tightly coupled to recently fixed and exported particulate organic matter (POC; Griffin and Druffel, 1989; Roark et al., 2005; Sherwood et al., 2005). Radiocarbon content of the calcite and gorgonin fractions therefore provide direct measures of seawater ^{14}C both at depth and in the overlying surface waters, respectively. The difference in ^{14}C age between surface and subsurface waters may then be used to assess the extent of vertical mixing of the water column.

In this paper, we examine radiocarbon variability in Northwest Atlantic slope waters using deep-sea gorgonians. Records of pre and post bomb- ^{14}C are generated for surface and upper intermediate slope water masses along a latitudinal gradient from 42°N to 60°N . Additional measurements from recent and subfossil specimens are used to assess vertical ^{14}C gradients in the upper 2000 m of the water column over the last 1200 years.

2. Samples

Specimens were collected with the remotely operated vehicle *ROPOS* and as fisheries bycatch (Fig. 1). A live specimen of *Keratoisis ornata* was collected from the southwest Grand Banks (specimen 1343) at 713 m depth. Subfossil *K. ornata* were collected from Baffin Bay (1298; 1008 m), Davis Strait (715; 923 m), Hudson Strait (1448, 1449; 1193 m), southwest Grand Banks (2460; 580 m) and Sable Gully (2431; 1826 m). *Primnoa*

resedaeformis was collected from Hudson Strait (1525-1, 1525-3, 1525-10; 414m) and Northeast Channel, off Southwest Nova Scotia (COHPS2001-1; 250-475 m). An additional 7 samples of *P. resedaeformis* (DFO-2002-con5A1, HUD-2001-055-VG13, HUD-2001-055-VG15, NED-2002-037-1A, NED-2002-037-5-1, ROPOS-639009, ROPOS-6400013; hereafter collectively referred to as S05) were collected from the Northeast Channel, as described earlier (Sherwood et al., 2005). A table of all samples, with dating and radiocarbon results is provided in the supplementary appendix.

3. Analytical Methods

K. ornata secretes a skeleton consisting of gorgonin nodes and calcite internodes (Noé and Dullo, 2006). Skeletons were sectioned longitudinally to facilitate sampling of coeval gorgonin and calcite samples from the same growth layer across the node-internode boundary. To generate timeseries $\Delta^{14}\text{C}$ records, samples were milled along transects from the outer margin to the central core, in increments of 0.3 – 0.9 mm, using a micromill fitted with a 0.3 mm diameter bit. *P. resedaeformis* secretes annual rings of calcite and gorgonin towards the inner part of the axial skeleton, enveloped by a crust of massive calcite in older specimens (Fig. 2A). Gorgonin samples were isolated by dissolving skeletal sections in 5% HCl and peeling apart the annual growth rings (Specimens 1525-1, 1525-3, 1525-10). Coeval samples of calcite were isolated from an adjacent section by oxidizing in a 50:50 solution of 30% H_2O_2 and 1N NaOH for 3 weeks (Specimen 1525-3). In a larger specimen of *P. resedaeformis* (COHPS2001-1) calcite samples were milled from a transect of the calcite crust.

For ^{14}C analyses, CO_2 aliquots evolved from calcite and decalcified gorgonin samples were reduced to graphite in the presence of iron catalyst. Radiocarbon measurements were performed on graphite targets at the Center for Accelerator Mass Spectrometry, Lawrence Livermore National Laboratory. Results include a background and $\delta^{13}\text{C}$ correction and are reported as $\delta^{14}\text{C}$ according to Stuiver and Polach (1977). Data for recent, known-age samples are also reported as age-corrected $\delta^{14}\text{C}$ (Stuiver and Polach, 1977) for easier comparison to seawater $\delta^{14}\text{C}$ data.

4. Dating Methods

Recently living corals were dated by one of 2 means. Young *P. resedaeformis* specimens lacking a calcite crust were dated by counting annual growth rings in transverse section. Ring counts were made by 3 different counters, to determine a mean calendar age ($\pm 1\sigma$) for each sampled growth ring, as described in Sherwood et al. (2005). An older *P. resedaeformis* (COHPS2001-1) and a *K. ornata* (1343) were dated with ^{210}Pb . Adjacent sections to those used for ^{14}C analyses were cut into 5-8 sub-samples, each weighing about 1 g. Sub-samples were crushed in an agate mortar, and the powder was oxidized in 30% H_2O_2 held at pH 8 by addition of 1N NH_4OH , then washed with de-ionized water and dried at 60°C . Measurement of ^{210}Pb was done by alpha spectrometry of its daughter product, ^{210}Po (Flynn, 1968). The ^{210}Pb -derived growth rate and chronological tie-in points defined skeletal chronology (Fig. 2).

Subfossil *K. ornata* specimens were dated by conventional ^{14}C dating of the gorgonin fraction. Raw ^{14}C ages were calibrated with the CALIB program (Stuiver and Reimer,

1993, version 5) using the Marine04 calibration (Hughen et al., 2004). A correction for local variation in the marine reservoir age (ΔR ; Stuiver and Braziunas, 1993) was applied, based on data from recent, known-age specimens presented herein. Marine reservoir ages are expressed either as $R(t)$ or ΔR (Stuiver et al., 1986). $R(t)$ is defined as the difference in ^{14}C years between a regional water mass and the ‘global’ (Northern Hemisphere) atmosphere. ΔR is the difference in ^{14}C years between a regional surface ocean and the modeled ‘global’ surface ocean (Stuiver et al., 1986). To first approximation, ΔR is time independent and is therefore the preferred method of correcting for the reservoir age of marine samples (Stuiver et al., 1986; Reimer and Reimer, 2001). ΔR is calculated by subtracting from the conventional ^{14}C age of a known-age marine sample the Marine04 model age for that calendar year. The Marine04 calibration and ΔR reflect the ^{14}C of surface waters. Because gorgonin reflects surface waters in terms of ^{14}C (Roark et al. 2005; Sherwood et al. 2005), only this fraction was used for ΔR calculations and age calibrations.

5. Results

Paired gorgonin and calcite $\Delta^{14}\text{C}$ records spanning pre- and post-nuclear bomb eras were generated for Hudson Strait, Grand Banks and Northeast Channel (Fig. 3). The $\Delta^{14}\text{C}$ content of gorgonin represents that of surface water, as indicated by good agreement with contemporaneous surface water values extracted from nearby TTO and WOCE stations. In all 3 records, bomb- ^{14}C began to increase around the year 1958. This validates our dating accuracy as 1958 ± 2 marked the year of initial increase in bomb- ^{14}C in the mixed layer of the oceans (Grottoli and Eaken, 2007). The records from Hudson Strait and

Grand Banks were similar: pre-bomb, age-corrected $\Delta^{14}\text{C}$ averaged $-68 \pm 3 \text{ ‰}$ (pooled mean, 1σ , $n = 10$) and bomb- ^{14}C peaked at around $+45 \text{ ‰}$ in the early 1980s. At Northeast Channel, pre-bomb values averaged slightly lower ($-75 \pm 5 \text{ ‰}$, 1σ , $n = 5$) and bomb- ^{14}C peaked at $+80 \text{ ‰}$ in 1970. No long term trends during the pre-bomb era were evident at any of the sites.

The $\Delta^{14}\text{C}$ content of calcite represents the $\Delta^{14}\text{C}$ of upper intermediate water at the depth where the corals were living (414 m, 713 m, and 250-475 m respectively for Hudson Strait, Grand Banks, and Northeast Channel; Fig. 3). At Hudson Strait and Grand Banks, intermediate water pre-bomb, age-corrected $\Delta^{14}\text{C}$ values averaged $-64 \pm 4 \text{ ‰}$ (pooled mean, 1σ , $n = 6$), within error of the corresponding surface water values. No long term trends were apparent during the pre-bomb era. At Northeast Channel, values were much more negative and oscillated quasi-decadally between -80 and -100 ‰ . Relative to surface waters, intermediate water bomb- ^{14}C signals were damped and lagged by varying amounts. Intermediate water bomb- ^{14}C appeared damped by approximately 10 ‰ at Hudson Strait and 80 ‰ at Northeast Channel, but more data are needed to resolve the signals at these sites. At Grand Banks, the intermediate water signal was better resolved by more data points and lagged the surface water signal by at least 20 years as $\Delta^{14}\text{C}$ had not peaked as of the year 2001.

In Fig. 4 we compare our bomb- ^{14}C records with two previously published records obtained from otoliths extracted from fish of age 0-3 years (Campana et al., 2008). One of these records was derived from otoliths of Greenland halibut (*Reinhardtius*

hippoglossoides) collected from the northern and western margins of the Labrador Sea (western Greenland, Davis Strait and Labrador shelf areas) from an average depth of 300 m. This record is most similar to our intermediate water data from Hudson Strait, and slightly depleted relative to our combined Hudson Strait and Grand Banks surface water data. The second otolith record was derived from haddock (*Melanogrammus aeglefinus*), redfish (*Sebastes* spp.) and yellowtail flounder (*Limanda ferruginea*) collected from the shelf waters of the southern Grand Banks. This record is more similar to our Northeast Channel surface water record.

Radiocarbon measurements of known-age samples from before AD 1950 are important for constraining the marine reservoir age. Table 1 shows local reservoir ages, $R(t)$, calculated from known-age, pre-bomb coral ^{14}C data. Values of $R(t)$ were statistically equal overall all regions and depths ($T = 6.55 < 11.07 = \chi^2_2; 0.05$; Ward and Wilson, 1978) with a weighted mean of 420 ± 20 ^{14}C years (1σ , $n = 6$). Even though the values were statistically equal, the reservoir age for intermediate waters at the Northeast Channel was notably older at 600 ± 95 (1σ , $n = 3$). Values of ΔR were calculated separately for the surface waters using gorgonin samples. Again, values were statistically equal ($T = 0.15 < 5.99 = \chi^2_2; 0.05$), so we computed a weighted mean of $\Delta R = 135 \pm 20$ (1σ , $n = 3$), representing surface slopewaters of the Northwest Atlantic, from Northeast Channel to offshore Hudson Strait. Similar ΔR values have been reported for the adjacent shelf and coastal waters in the Marine Reservoir Correction Database (Reimer and Reimer, 2001). For example, for coastal Labrador $\Delta R = 150 \pm 67$ (weighted mean, 1σ , n

= 26) and for coastal and shelf waters from the Gulf of Maine to the southern Grand Banks $\Delta R = 87 \pm 64$ (n = 33).

Coeval gorgonin and calcite samples from live-collected and subfossil corals were used to assess vertical ^{14}C gradients over a latitudinal range of 42-68°N and over the last 1200 years (Table 2). From one of the subfossil corals, we generated a continuous record of ^{14}C across the calcite internode, indicating a lifespan of 200 years (Fig. 5). We attempted to date the subfossil specimens independently using U/Th dating; however, femtogram concentrations of Th made it difficult to calculate reliable U/Th ages. Instead, we used the ^{14}C age of the gorgonin fraction to calculate calendar age, using the 135 ± 20 year ΔR correction established above. By differencing the $\Delta^{14}\text{C}$ of paired gorgonin and calcite samples, we obtained vertical gradients in ^{14}C age (and corresponding $\Delta^{14}\text{C}$, uncorrected for age at formation) of the water column (Fig. 6). Positive values of the difference in ^{14}C age represent a normally stratified water column, with younger waters overlying older waters. The most positive value was found at Northeast Channel, where subsurface waters are older than surface waters by an average of 125 ^{14}C years. A positive value was also found at the next most northerly location, the Sable Gully. Northward of the Scotian Slope, values averaged around zero or were negative. There were no apparent long term trends in vertical $\Delta^{14}\text{C}$ gradients over the past 1200 years (Fig. 6). For example, excluding the Northeast Channel (S05/COHPS2001-1) and Sable Gully (2431) samples, all of the remaining samples were within error of each other in terms of the difference between surface and intermediate water ^{14}C ages (Fig. 6).

6. Discussion

Slope waters of the Northwest Atlantic comprise a mixture of different water masses. In the northern Labrador Sea, a 100 m deep surface layer forms during the summer. In winter, convective mixing homogenizes the water column to ~1500 m, forming an upper, recently ventilated layer of Labrador Sea Water (Azetsu-Scott et al., 2005). Because of mixing, the vertical $\Delta^{14}\text{C}$ gradient near Hudson Strait is minimal: pre-bomb values are identical between 0 and 400 m, and the bomb- ^{14}C signal at 400 m is only slightly depleted relative to the surface signal (Fig. 3A). A previously published bomb- ^{14}C record based on Greenland Halibut otoliths collected from the margins of the Labrador Sea (Campana et al., 2008) is most similar to our 400 m deep Hudson Strait data because the fish were collected at an average depth of 300 m (Fig. 4). Overall, vertical mixing dampens and lags bomb- ^{14}C records in the Labrador Sea relative to our more southerly record from the Northeast Channel (Fig. 4) and relative to other regions of the North Atlantic, where bomb- ^{14}C peaked between +80 and +150 ‰ in the early 1970s (Druffel, 1980; Kalish, 1993; Weidman and Jones, 1993; Campana et al., 2008).

The offshore branch of the Labrador Current transports part of the upper Labrador Sea Water as Labrador Slope Water (LSW) southward from Hudson Strait along the continental slope of Newfoundland and Labrador. At 43°N, it bifurcates and part of it continues westward along the southern flank of the Grand Banks (Drinkwater, 1996). It takes < 1 year for the Labrador Current to transit from Hudson Strait to the Grand Banks (Lazier and Wright, 1993); therefore, surface water $\Delta^{14}\text{C}$ records at the 2 areas are nearly identical (Fig. 3A,B). The 700 m deep record at the Grand Banks reflects a deeper layer

of LSW in which bomb- ^{14}C lags that of surface waters by at least 20 years (Fig. 3B).

During the pre-bomb era, however, the vertical $\Delta^{14}\text{C}$ gradient from 0 – 700 m remained near zero.

A previously published bomb- ^{14}C record from nearby shelf waters of the southwest Grand Banks, based on otoliths of age 1-3 haddock (*Melanogrammus aeglefinus*), redfish (*Sebastes* spp.) and yellowtail flounder (*Limanda ferruginea*) (Campana et al., 2008), showed a more rapid increase in bomb- ^{14}C , virtually identical in timing and amplitude to our Northeast Channel surface water record (Fig. 4). This record primarily reflects Labrador Shelf Waters (LShW) of the inshore branch of the Labrador Current (Houghton and Fairbanks, 2001). Compared with the slope region, vertical mixing on the shelf is limited by bathymetry to < 250m, thus leading to more rapid equilibration of LShW with atmospheric bomb- ^{14}C . These results highlight important differences in bomb- ^{14}C signals from adjacent regions.

The Labrador Current carries LSW further westward toward the Nova Scotia slope where it forms a front with Warm Slope Water (WSW) originating from the south. WSW occupies the region between the shelf break and the north wall of the Gulf Stream. The frontal boundary between LSW and WSW moves along-slope between approx. 69°W and 57°W, in response to basin-scale forcing associated with the modal state North Atlantic Oscillation (NAO; Petrie and Drinkwater, 1993; Greene and Pershing, 2003). Thus, during positive years of the NAO the upper slope region off Nova Scotia is occupied by WSW; during negative states it is occupied by LSW.

285
286 The pre-bomb vertical $\Delta^{14}\text{C}$ gradient at Northeast Channel is much higher than anywhere
287 else further north over the last 1200 years (Fig. 6). This is caused by the presence of
288 older, ^{14}C depleted water at 250-475 m at the Northeast Channel. Negative excursions to -
289 100 ‰ during the pre-bomb era cannot be associated with the presence of LSW, based on
290 values of -70 ‰ upstream at Grand Banks and Hudson Strait (Fig. 3). Instead, the
291 negative values must originate from WSW. From nutrient data, WSW is thought to mix
292 with Antarctic Intermediate Water (AAIW), located at ~1000 m below the Gulf Stream,
293 via isopycnal shoaling (Richardson, 1977; Atkinson, 1983; Csanady and Hamilton,
294 1988). AAIW has a $\Delta^{14}\text{C}$ signature of -110 ‰ (Broecker et al., 1960). Mixing with
295 AAIW would impart a more negative $\Delta^{14}\text{C}$ signature to WSW, as previously suggested
296 for the slope waters south of the Northeast Channel (Tanaka et al., 1990). If WSW is the
297 source of negative $\Delta^{14}\text{C}$ excursions, then the $\Delta^{14}\text{C}$ record for subsurface Northeast
298 Channel may reflect NAO-driven shifts in the relative dominance of younger LSW vs.
299 older WSW. The resolution of our ^{210}Pb -dated record does not permit a timeseries
300 correlation with the NAO; however, future developments in precise U/Th dating of
301 gorgonian calcites may allow for the development of detailed, long term proxy records of
302 slope water movements here, and in other dynamic regions.

303

304 **7. Conclusions**

305 Deep-sea corals present new archives of seawater ^{14}C , particularly in high latitude and/or
306 deep-water environments where proxy data generally are lacking. One of the benefits of
307 deep-sea gorgonians versus scleractinian corals is the ability to generate both surface and

deep-water ^{14}C chronologies from the same skeleton. From ^{14}C measurements on both fractions, we determined new estimates of radiocarbon reservoir ages of Northwest Atlantic slopewaters, which could be used for more precise ^{14}C dating of cores recovered from this area. From measurements on co-eval gorgonin and calcite fractions we generated new data on seawater vertical ^{14}C gradients over the last 1200 years. While there were no apparent changes in vertical ^{14}C gradients over this time period, the most significant finding was the presence of a ^{14}C -depleted water mass which invades the southern region of the Scotian Slope on decadal timescales. These findings demonstrate the utility of deep-sea gorgonians in tracking water mass movements in oceanographically dynamic regions.

Acknowledgements

We gratefully acknowledge Derek Jones, Pal Mortensen, the fisheries observers and officers and crew of the CCGS *Hudson*, and *ROPOS* technicians for their assistance in acquiring samples. We also thank Kent Gilkinson and Vonda Wareham for logistical support, Steve Campana for use of the micromill, and Theo Pitsiavas, Jessie Tesolin and Christine Ward-Paige for counting growth rings. Finally, we thank Kumiko Azetsu-Scott, Richard Fairbanks and 2 anonymous reviewers for comments on earlier versions of this manuscript. This work was supported by the Canadian Department of Fisheries and Oceans IGP funds, and an NSERC postdoctoral fellowship to OAS. Radiocarbon analyses were performed under the auspices of the U.S. Department of Energy by the Lawrence Livermore National Laboratory under Contract No. DE-AC52-07NA27344.

References

Adkins, J.F., H. Cheng, E.A. Boyle, E.R.M. Druffel, and R.L. Edwards (1998), Deep-sea coral evidence for rapid change in ventilation of the deep North Atlantic 15,400 years ago. *Science*, 280, 725-728.

Adkins, J.F., S. Griffin, M. Kashgarian, H. Cheng, E.R.M. Druffel, E.A. Boyle, R. L. Edwards, and C.C. Shen (2002), Radiocarbon dating of deep-sea corals, *Radiocarbon*, 44, 567-580.

Atkinson, L.P. (1983), Distribution of Antarctic Intermediate Water over the Blake Plateau, *J. Geophys. Res.*, 88 (C8), 4699-4704.

Azetsu-Scott, K., E.P. Jones, and R.M. Gershey (2005), Distribution and ventilation of water masses in the Labrador Sea inferred from CFCs and carbon tetrachloride, *Mar. Chem.*, 94, 55-66.

Broecker, W.S., R. Gerard, M. Ewing, and B.C. Heezen (1960), Natural radiocarbon in the Atlantic Ocean, *J. Geophys. Res.*, 65(a), 2903-2931.

Broecker, W. S., T.-H. Peng, G. Ostlund, and M. Stuiver (1985), The distribution of bomb radiocarbon in the ocean, *J. Geophys. Res.*, 90, 6953–6970.

Bondevik, S., H.H. Birks, S. Gulliksen, and J. Mangerud (1999) Late Weichselian Marine ¹⁴C Reservoir Ages at the Western Coast of Norway. *Quat. Res.* 52, 104-114.

355

356 Campana, S.E., L.J. Natanson, and S. Myklevoll (2002), Bomb dating and age
 357 determination of large pelagic sharks, *Can. J. Fish. Aquat. Sci.*, *59*, 450-455.

358

359 Campana, S.E., J.M. Casselman, and C.M. Jones (2008) Bomb radiocarbon chronologies
 360 in the Arctic, with implications for the age validation of lake trout (*Salvelinus*
 361 *namaycush*) and other Arctic species. *Can. J. Fish. Aquat. Sci.*, *65*, 733-743.

362

363 Cao, L., R.G. Fairbanks, R.A. Mortlock, and M.J. Risk (2007), Radiocarbon reservoir age
 364 of high latitude North Atlantic surface water during the last deglacial, *Quat. Sci. Rev.*, *26*,
 365 732-742.

366

367 Cember, R. (1989), Bomb radiocarbon in the Red Sea: a medium-scale gas exchange
 368 experiment. *J. Geophys. Res.*, *94*, 2111-2123.

369

370 Cheng, H., J.A. Adkins, R.L. Edwards, and E.A. Boyle (2000), U-Th dating of deep-sea
 371 corals. *Geochim. Cosmochim. Acta.*, *64*, 2401-2416.

372

373 Csanady, G.T., and P. Hamilton (1988), Circulation of slopewater. *Cont. Shelf Res.*, *8*,
 374 565-624.

375

376 Drinkwater, K.F. (1996), Atmospheric and oceanic variability in the Northwest Atlantic
 377 during the 1980s and early 1990s, *J. Northw. Atl. Fish. Sci.*, *18*, 77-97.

378

379 Druffel, E.R.M. (1980), Radiocarbon in Annual Coral Rings of Belize and Florida,
 380 *Radiocarbon* 22, 363–371.
 381
 382 Druffel, E.R.M. (1997), Pulses of rapid ventilation in the North Atlantic surface ocean
 383 during the past century, *Science*, 275, 1454-1457.
 384
 385 Eltgroth, S.F., J.F. Adkins, L.F. Robinson, J. Southon, and M. Kashgarian (2006) A deep-
 386 sea coral record of North Atlantic radiocarbon through the Younger Dryas: Evidence for
 387 intermediate water/deepwater reorganization. *Paleoceanography*, 21, PA4207,
 388 doi:10.1029/2005PA001192.
 389
 390 Fallon, S.J., T.P. Guilderson, and K. Caldeira (2003), Carbon isotope constraints on
 391 vertical mixing and air-sea CO₂ exchange, *Geophys. Res. Lett.*, 30(24), 2289,
 392 doi:10.1029/2003GL018049,
 393
 394 Flynn, W.W. (1968), The determination of low levels of polonium-210 in environmental
 395 materials. *Anal. Chim. Acta.*, 43, 221–227.
 396
 397 Frank, N., M. Paterne, L. Ayliffe, T. van Weering, J.-P. Henriët, and D. Blamart (2004),
 398 Eastern North Atlantic deep-sea corals: tracing upper intermediate water $\Delta^{14}\text{C}$ during the
 399 Holocene, *Earth Plan. Sci. Lett.*, 219, 297-309.
 400

401 Goldstein, S.J., D.W. Lea, S. Chakraborty, M. Kashgarian, and M.T. Murrell (2001),
402 Uranium-series and radiocarbon geochronology of deep-sea corals: implications for
403 Southern Ocean ventilation rates and the oceanic carbon cycle, *Earth Plan. Sci. Lett.*,
404 *193*, 167-182.

405

406 Greene, C.H., and Pershing, A.J. (2003), The flip side of the North Atlantic Oscillation
407 and modal shifts in slope-water circulation, *Limnol. Oceanogr.*, *48*(1), 319-322.

408

409 Griffin, S., and E. R. M. Druffel (1989), Sources of carbon to deep-sea corals,
410 *Radiocarbon*, *55*, 533– 542.

411

412 Grottoli, A.G., and C.M. Eakin (2007) A review of modern coral $\delta^{18}\text{O}$ and $\Delta^{14}\text{C}$ proxy
413 records, *Earth Sci. Rev.*, *81*, 67-91.

414

415 Guilderson, T.P., D.P. Schrag, M. Kashgarian, and J. Southon (1998), Radiocarbon
416 variability in the western equatorial Pacific inferred from a high resolution coral record
417 from Nauru Island. *J. Geophys. Res.*, *103*, 24641-24650.

418

419 Guilderson, T.P., D.P. Schrag, and M.A. Cane (2004), Surface water mixing in the
420 Solomon Sea as documented by a high-resolution coral ^{14}C record, *J. Climate*, *17*, 1147–
421 1156.

422

423 Guilderson, T.P., J.E. Cole, and J.R. Southon (2005), Pre-bomb $\delta^{14}\text{C}$ variability and the
 424 Suess effect in Cariaco Basin surface waters as recorded in hermatypic corals,
 425 *Radiocarbon*, 47, 57–65.
 426
 427 Houghton, R.W., and Fairbanks, R.G. (2001), Water sources for Georges Bank, *Deep-Sea*
 428 *Res. II*, 48, 95-114.
 429
 430 Hughen, K.A., M.G.L. Baillie, E. Bard, A. Bayliss, J.W. Beck, C.J.H. Bertrand, P.G.
 431 Blackwell, C.E. Buck, G.S. Burr, K.B. Cutler, P.E. Damon, R.L. Edwards, R.G.
 432 Fairbanks, M. Friedrich, T.P. Guilderson, B. Kromer, F.G. McCormac, S.W. Manning, C.
 433 Bronk Ramsey, P.J. Reimer, R.W. Reimer, S. Remmele, J.R. Southon, M. Stuiver, S.
 434 Talamo, F.W. Taylor, J. van der Plicht, and C.E. Weyhenmeyer (2004), Marine 04
 435 Marine radiocarbon age calibration, 26 - 0 ka BP, *Radiocarbon*, 46, 1059-1086.
 436
 437 Ingram, B.L., and J.R. Southon (1996) Reservoir ages in Eastern Pacific Coastal and
 438 Estuarine Waters. *Radiocarbon*, 38, 573-582.
 439
 440 Kalish, J.M. (1993), Pre- and post-bomb radiocarbon in fish otoliths. *Earth Plan. Sci.*
 441 *Lett.*, 114, 549-554.
 442
 443 Kerr, L.A., A.H. Andrews, K. Munk, G.M. Cailliet, K.H. Coale, T.A. Brown, and B.R.
 444 Frantz (2005), Age validation of quillback rockfish (*Sebastes maliger*) using bomb
 445 radiocarbon, *Fish. Bull.*, 103, 97-107.

446

447 Key, R.M., A. Kozyr, K. Lee, R. Wanninkhof, J.L. Bullister, R.A. Feely, F.J. Millero, C.

448 Mordy, and T.-H. Peng (2004), A global ocean carbon climatology: Results from Global

449 Data Analysis Project (GLODAP). *Global Biogeochem. Cycles.*, 18, GB4031.

450 doi:10.1029/2004GB002247.

451

452 Kilada, R.W., S.E. Campana, and D. Roddick (2007), Validated age, growth, and

453 mortality estimates of the ocean quahog (*Arctica islandica*) in the western Atlantic, *ICES*

454 *J. Mar. Sci.*, 64, 31-38.

455

456 Lazier, J.R.N., and D.G. Wright (1993), Annual velocity variations in the Labrador

457 Current, *J. Phys. Oceanogr.* 23, 659-678.

458

459 Mangini, A., M. Lomitschka, R. Eichstadter, N. Frank, S. Vogler (1998), Coral provides

460 way to age deep water. *Nature*, 392, 347-348.

461

462 Noé, S.U., and W.-Chr. Dullo (2006), Skeletal morphogenesis and growth mode of

463 modern fossil and deep-water isidid gorgonians (Octocorallia) in the West Pacific (New

464 Zealand and Sea of Okhotsk), *Coral Reefs*, 25, 303-320.

465

466 Östlund, H.G., H. Craig, W.S. Broecker, and D. Spencer (1987), GEOSECS Atlantic,

467 Pacific, and Indian Ocean Expeditions. Vol. 7, National Science Foundation 200 pp.

468

469 Petrie, B., and K. Drinkwater (1993), Temperature and salinity variability on the Scotian
 470 Shelf and in the Gulf of Maine 1945-1990. *J. Geophys. Res.* *98 (C11)*, 20079-20089.
 471
 472 Richardson, P.L. (1977), On the crossover between the Gulf Stream and the Western
 473 Boundary Undercurrent. *Deep-Sea Res.*, *24*, 139-159.
 474
 475 Reimer, P.J., and R.W. Reimer (2001) A Marine reservoir correction database and on-line
 476 interface. *Radiocarbon*, *43*, 461-463. Available online at <http://intcal.qub.ac.uk/marine/>.
 477
 478 Reimer, P.J., M.G.L. Baillie, E. Bard, A. Bayliss, J.W. Beck, C. Bertrand, P.G.
 479 Blackwell, C.E. Buck, G. Burr, K.B. Cutler, P.E. Damon, R.L. Edwards, R.G. Fairbanks,
 480 M. Friedrich, T.P. Guilderson, K.A. Hughen, B. Kromer, F.G. McCormac, S. Manning,
 481 C. Bronk Ramsey, R.W. Reimer, S. Remmele, J.R. Southon, M. Stuiver, S. Talamo, F.W.
 482 Taylor, J. van der Plicht, and C.E. Weyhenmeyer (2004), IntCal04 Terrestrial
 483 radiocarbon age calibration, 26 - 0 ka BP. *Radiocarbon*, *46*, 1029-1058.
 484
 485 Roark, E.B., T.P. Guilderson, S. Flood-Page, R.B. Dunbar, B.L. Ingram, S.J. Fallon, and
 486 M. McCulloch (2005), Radiocarbon-based ages and growth rates of bamboo corals from
 487 the Gulf of Alaska, *Geophys. Res. Lett.*, *32*, L04606, doi:10.1029/2004GL021919.
 488
 489 Roark, E.B., T.P. Guilderson, R.B. Dunbar, B.L. Ingram (2006) Radiocarbon-based ages
 490 and growth rates of Hawaiian deep-sea corals. *Mar. Ecol. Prog. Ser.*, *327*, 1-14.
 491

492 Robinson, L.F., J.F. Adkins, L.D. Keigwin, J. Southon, D.P. Fernandez, S.-L. Wang, and
 493 D.S. Scheirer (2005), Radiocarbon variability in the Western North Atlantic during the
 494 last deglaciation, *Science*, *310*, 1469-1473.
 495
 496 Schlitzer, R. (1996), Ocean Data View, <http://odv.awi.de>.
 497
 498 Schröder-Ritzrau, A., A. Mangini, and M. Lomitschka (2003), Deep-sea corals evidence
 499 periodic reduced ventilation in the North Atlantic during the LGM/Holocene transition,
 500 *Earth Plan. Sci. Lett.*, *216*, 399-410.
 501
 502 Sikes, E.L., S.N. Burgess, R. Grandpre, and T.P. Guilderson (2008), Assessing modern
 503 deep-water ages in the New Zealand region using deep-water corals. *Deep-Sea Res. I*, *55*,
 504 38-49.
 505
 506 Sherwood, O.A., D.B. Scott, M.J. Risk, and T.P. Guilderson (2005), Radiocarbon
 507 evidence for annual growth rings in the deep-sea octocoral *Primnoa resedaeformis*. *Mar.*
 508 *Ecol. Prog. Ser.*, *301*, 129-134.
 509
 510 Sherwood, O.A., D.B. Scott and M.J. Risk (2006), Late Holocene radiocarbon and
 511 aspartic acid racemization dating of deep-sea octocorals. *Geochim. Cosmochim. Acta*, *70*,
 512 2806-2814.
 513

514 Stuiver, M. and H.A. Polach (1977), Discussion: reporting of ^{14}C data. *Radiocarbon*, 19,
 515 355-363.
 516
 517 Stuiver, M., and T.F. Braziunas (1993), Modeling atmospheric ^{14}C influences and ^{14}C
 518 ages of marine samples to 10,000 BC, *Radiocarbon*, 35, 137-189.
 519
 520 Stuiver, M., and Reimer, P.J. (1993), Extended ^{14}C database and revised CALIB
 521 radiocarbon calibration program, *Radiocarbon*, 35, 215-230. (version 5,
 522 <http://radiocarbon.pa.qub.ac.uk/calib/>).
 523
 524 Stuiver, M., G.W. Pearson, and T. Braziunas (1986), Radiocarbon age calibration of
 525 marine samples back to 9000 Cal YR BP. *Radiocarbon*, 28, 980-1021.
 526
 527 Tanaka, N., M.C. Monaghan, and K.K. Turekian (1990), $\delta^{14}\text{C}$ balance for the Gulf of
 528 Maine, Long Island Sound and the Middle Atlantic Bight: Evidence for the extent of
 529 Antarctic Intermediate Water contribution. *J. Mar. Res.* 48, 75-87.
 530
 531 Ward, G.K., and S.R. Wilson (1978), Procedures for comparing and combining
 532 radiocarbon age determinations: a critique, *Archaeometry*, 20(1), 19-31.
 533
 534 Weidman, C.R., and G.A. Jones (1993), A shell-derived time history of bomb ^{14}C on
 535 Georges Bank and its Labrador Sea implications, *J. Geophys. Res.*, 98 (C8), 14577-
 536 14588.

Table 1: Summary of pre-bomb ^{14}C ages of gorgonin and calcite fractions of recent, known-age corals and corresponding $R(t)'$ and ΔR values. Values in brackets are 1σ errors.

| Coral ID | Band or subsample | Year AD | CAMS # | ^{14}C Age (years) | IntCal Age ^d | $R(t)'$ | Marine04 Age ^e | ΔR |
|--|-------------------|-------------------------|--------|-----------------------------|-------------------------|----------|---------------------------|------------|
| Hudson Strait, 60.5°N/61.4°W, 275-450 m | | | | | | | | |
| <i>Gorgonin</i> | | | | | | | | |
| 1525-3 | 53 | 1925 (8) ^b | 131411 | 610 (25) | 132 (7) | 478 (26) | 451 (23) | 159 (34) |
| 1525-1 | 31 | 1946 (2) ^b | 131423 | 585 (25) | 188 (8) | 397 (26) | 464 (23) | 121 (34) |
| 1525-3 | 32 | 1949 (7) ^b | 131410 | 585 (30) | 197 (9) | 388 (31) | 468 (24) | 117 (38) |
| | | | | Mean (s.d.) | | 421 (50) | | 132 (23) |
| <i>Calcite</i> | | | | | | | | |
| 1525-3 | C5 | 1941(10) ^b | 132208 | 555 (30) | 176 (8) | 379 (31) | | |
| Grand Banks, 44.13°N/52.93°W, 713 m | | | | | | | | |
| <i>Gorgonin</i> | | | | | | | | |
| 1343 | G19 | 1943 (10) ^c | 131278 | 570 (25) | 182 (8) | 388 (26) | 462 (23) | 108 (34) |
| 1343 | G25 | 1934 (12) ^c | 131279 | 605 (30) | 157 (7) | 448 (31) | 456 (23) | 149 (38) |
| 1343 | G32 | 1925 (13) ^c | 131280 | 585 (25) | 132 (7) | 453 (26) | 451 (23) | 134 (34) |
| 1343 | G37 | 1919 (14) ^c | 131281 | 590 (25) | 126 (7) | 464 (26) | 449 (23) | 141 (34) |
| 1343 | G43 | 1910 (15) ^c | 131282 | 675 (25) | 96 (7) | 579 (26) | 448 (23) | 227 (34) |
| 1343 | G52-53 | 1896 (18) ^c | 131382 | 575 (25) | 75 (7) | 500 (26) | 459 (23) | 116 (34) |
| 1343 | G58 | 1884 (20) ^c | 131383 | 625 (30) | 103 (7) | 522 (31) | 470 (23) | 155 (38) |
| | | | | Mean (s.d.) | | 479 (61) | | 147 (39) |
| <i>Calcite</i> | | | | | | | | |
| 1343 | C9 | 1949 (10) ^c | 132003 | 560 (25) | 197 (9) | 363 (27) | | |
| 1343 | C11 | 1934 (12) ^c | 132004 | 525 (30) | 157 (7) | 368 (31) | | |
| 1343 | C15 | 1909 (16) ^c | 132005 | 590 (30) | 95 (7) | 495 (31) | | |
| 1343 | C17 | 1894 (18) ^c | 132006 | 525 (25) | 81 (7) | 444 (26) | | |
| 1343 | C19 | 1879 (21) ^c | 132007 | 605 (25) | 111 (7) | 494 (26) | | |
| | | | | Mean (s.d.) | | 433 (65) | | |
| NE Channel, 42.0°N/65.5°W | | | | | | | | |
| <i>Gorgonin</i> | | | | | | | | |
| S05: | | | | | | | | |
| NED-2002-037-1A ^a | 58 | 1947 (1) ^b | 111330 | 630 (35) | 193 (8) | 437 (36) | 466 (23) | 164 (42) |
| DFO-2002-con5A1 ^a | 37 | 1948 (4) ^b | 97103 | 620 (30) | 195 (9) | 425 (31) | 467 (23) | 153 (38) |
| DFO-2002-con5A1 ^a | 43 | 1942 (5) ^b | 97104 | 545 (30) | 179 (8) | 366 (31) | 461 (23) | 84 (38) |
| DFO-2002-con5A1 ^a | 50 | 1934 (6) ^b | 97105 | 595 (30) | 157 (7) | 438 (31) | 456 (23) | 139 (38) |
| DFO-2002-con5A1 ^a | 58 | 1924 (6) ^b | 97106 | 550 (30) | 131 (7) | 419 (31) | 451 (23) | 99 (38) |
| | | | | Mean (s.d.) | | 417 (30) | | 128 (35) |
| <i>Calcite</i> | | | | | | | | |
| COHPS-2001-1E | 1&2 | 1890 (22) ^c | 97759 | 640 (40) | 98 (7) | 542 (41) | | |
| COHPS-2001-1E | 3&4 | 1895 (21) ^c | 97760 | 700 (40) | 78 (7) | 622 (41) | | |
| COHPS-2001-1E | 5&6 | 1900 (19) ^c | 97761 | 850 (60) | 70 (7) | 780 (60) | | |
| COHPS-2001-1E | 7&8 | 1905 (17) ^c | 97762 | 680 (35) | 83 (7) | 597 (36) | | |
| COHPS-2001-1E | 9&10 | 1911 (16) ^c | 97763 | 770 (60) | 97 (7) | 673 (60) | | |
| COHPS-2001-1E | 11&12 | 1916 (15) ^c | 97764 | 705 (40) | 110 (7) | 595 (41) | | |
| COHPS-2001-1E | 13&14 | 1921 (13) ^c | 97765 | 625 (40) | 130 (7) | 495 (41) | | |
| COHPS-2001-1E | 15&16 | 1926 (110) ^c | 97766 | 785 (50) | 135 (7) | 650 (50) | | |
| COHPS-2001-1E | 17&18 | 1930 (10) ^c | 97767 | 695 (40) | 151 (7) | 544 (41) | | |
| COHPS-2001-1E | 19&20 | 1936 (8) ^c | 97768 | 835 (40) | 159 (8) | 676 (41) | | |
| COHPS-2001-1E | 21&22 | 1941 (7) ^c | 97769 | 625 (40) | 176 (8) | 449 (41) | | |
| | | | | Mean (s.d.) | | 602 (93) | | |

^a Data from Sherwood et al., 2005, 2006

^b Growth ring counted age

^c ^{210}Pb -dated age

^d Intcal04 model age (Reimer et al., 2004)

^e Marine04 model age (Hughen et al., 2004)

Table 2: Summary of recent (pre-1950) and subfossil samples, with paired radiocarbon data from coeval gorgonin and calcite fractions. All errors (in brackets) are $\pm 1\sigma$. Where $N > 1$, the mean $\pm 1\sigma$ of multiple samples are reported.

| Coral ID | Band or subsample | Skeletal fraction | N | $\Delta^{14}\text{C}$ (‰) | Diff. (‰) ^a | ^{14}C age (yrs) | Diff. (yrs) ^b | Cal Age (yrs AD) |
|--|-------------------|-------------------|---|---------------------------|------------------------|---------------------------|--------------------------|------------------------|
| Subfossil corals | | | | | | | | |
| <i>Baffin Bay, 67.93°N/59.45°W, 1008 m</i> | | | | | | | | |
| 1298 | G1 | gorgonin | 1 | -82 (3) | 9 (4) | 685 (25) | -75 (36) | 1750 (50) ^c |
| | C1 | calcite | 1 | -73 (2) | | 610 (25) | | |
| <i>Davis Strait, 63.53°N/58.75°W, 923 m</i> | | | | | | | | |
| 715 | G1 | gorgonin | 1 | -194 (2) | 0 (4) | 1735 (25) | -5 (39) | 780 (50) ^c |
| | C1 | calcite | 1 | -194 (3) | | 1730 (30) | | |
| <i>Hudson Strait, 60.6°N/60.38°W, 1193 m</i> | | | | | | | | |
| 1448 | G1 | gorgonin | 1 | -184 (2) | 7 (4) | 1640 (25) | -70 (35) | 900 (50) ^c |
| | C1 | calcite | 1 | -177 (3) | | 1570 (25) | | |
| 1449 | G1 to G6/7 | gorgonin | 6 | -181 (4) | 3 (7) | 1601 (39) | -32 (71) | 950 (50) ^c |
| | C1 to C6 | calcite | 6 | -178 (6) | | 1569 (59) | | |
| <i>Grand Banks, 44.83°N/54.47°W/ 578 m</i> | | | | | | | | |
| 2460 | G1 | gorgonin | 1 | -92 (3) | 0 (4) | 775 (30) | 0 (39) | 1670 (40) ^c |
| | C1 | calcite | 1 | -92 (3) | | 775 (25) | | |
| <i>Sable Gully, 43.68°N/58.82°W, 1826 m</i> | | | | | | | | |
| 2431 | G1 | gorgonin | 1 | -147 (3) | -5 (4) | 1280 (25) | 45 (35) | 1260 (30) ^c |
| | C1 | calcite | 1 | -152 (3) | | 1325 (25) | | |
| Recent corals | | | | | | | | |
| <i>Hudson Strait, 60.5°N/61.4°W, 414 m</i> | | | | | | | | |
| 1525-1 | G31 | gorgonin | 3 | -71 (1) | 4 (3) | 593 (14) | -38 (33) | 1940 (13) ^d |
| 1525-3 | G32, G53 | | | | | | | |
| 1525-3 | C5 | calcite | 1 | -67 (3) | | 555 (30) | | 1941 (10) ^d |
| <i>Grand Banks, 44.13°N/52.93°W, 713 m</i> | | | | | | | | |
| 1343 | G19 to G58 | gorgonin | 7 | -72 (4) | 4 (6) | 604 (37) | -43 (52) | 1916 (21) ^c |
| 1343 | 1343-C9 to C19 | calcite | 5 | -68 (4) | | 561 (37) | | 1913 (29) ^c |
| <i>NE Channel, 42.0°N/65.5°W, 275-450 m</i> | | | | | | | | |
| S05: | | | | | | | | |
| NED-2002-037-1A | G58 | gorgonin | 5 | -77 (5) | -14 (12) | 588 (39) | 125 (103) | 1939 (10) ^d |
| DFO-2002-con5A1 | G37 to G58 | | | | | | | |
| COHPS2001-1E | C13&14 to C21&22 | calcite | 5 | -91 (11) | | 713 (95) | | 1931 (8) ^c |

^a Calcite $\Delta^{14}\text{C}$ minus gorgonin $\Delta^{14}\text{C}$

^b Calcite ^{14}C age minus gorgonin ^{14}C age

^c ΔR -corrected Marine04 calibrated age; $\Delta\text{R} = 135 \pm 20$.

^d Growth ring counted age

^e ^{210}Pb -dated age

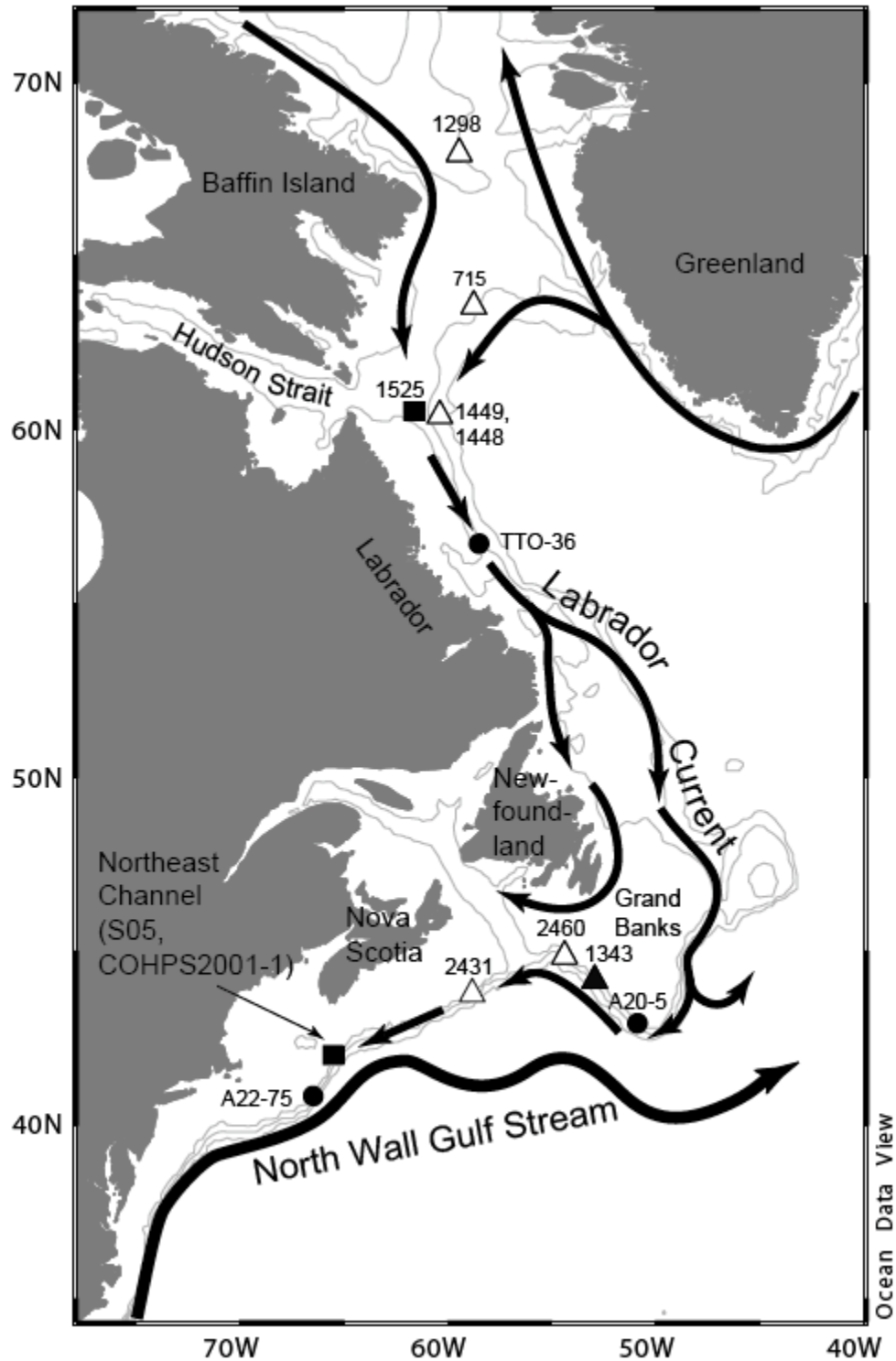


Fig. 1: Map of Northwest Atlantic region showing locations of coral samples. Closed triangle, recent *K. ornata*; open triangle, subfossil *K. ornata*, squares, recent *P. resedaeformis*. Also shown, nearby TTO and WOCE seawater stations extracted from the GLODAP dataset (circles; Key et al. 2004). Major surface currents indicated with arrows. Map drawn with ODV software (Schlitzer, 2006)

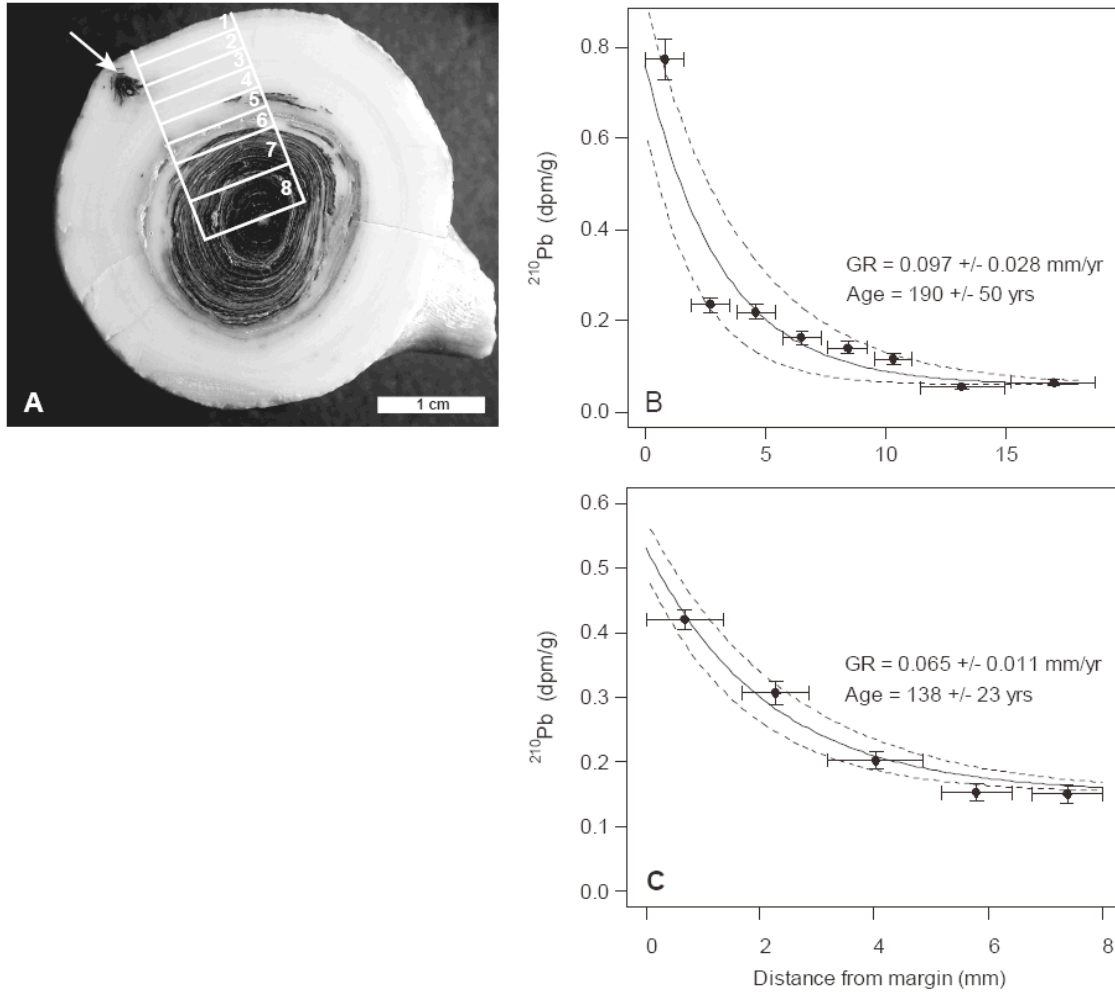
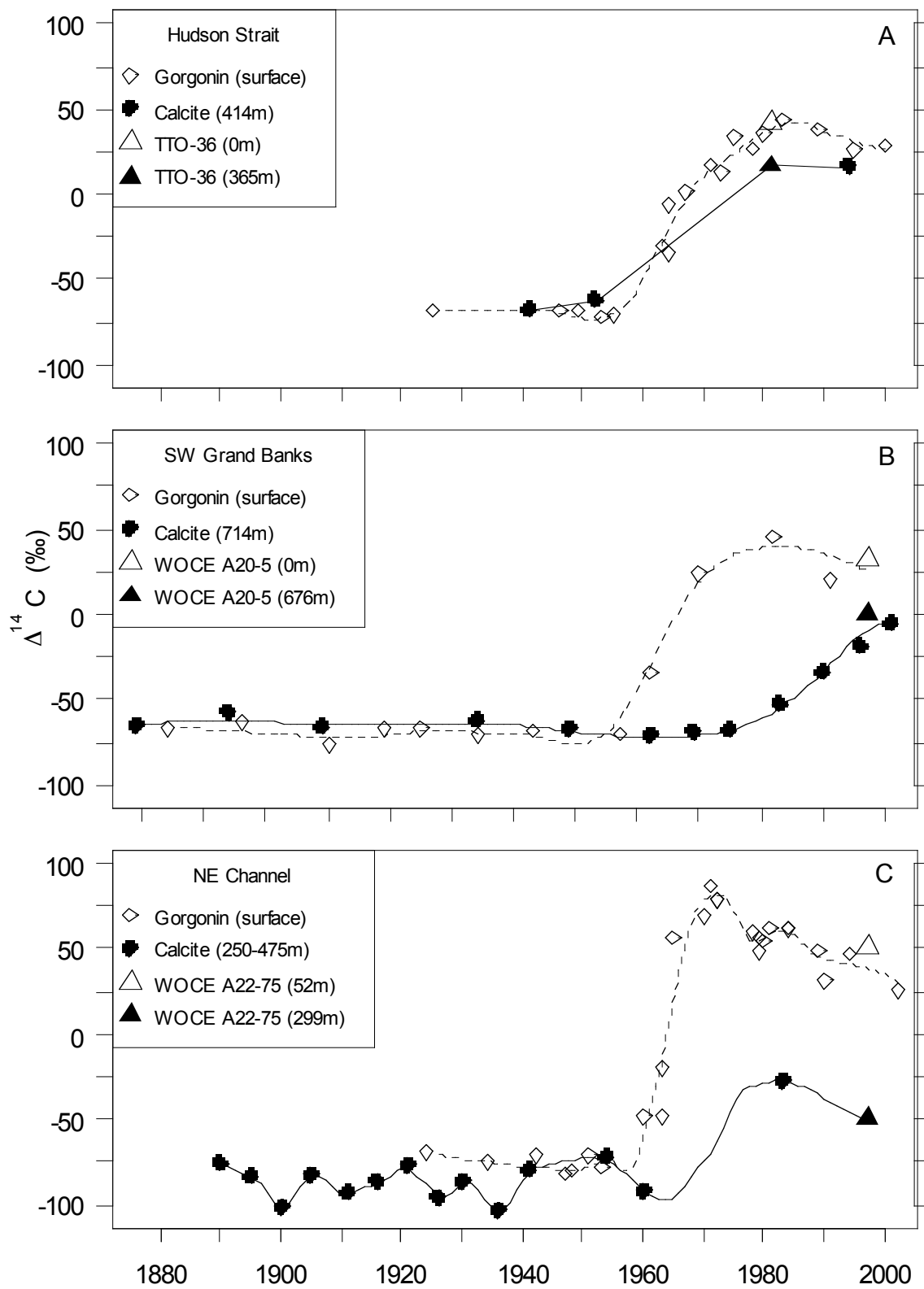


Fig. 2: (A) *P. resedaeformis* specimen COHPS2001-1 in transverse section, showing inner, annually banded gorgonin region overgrown by calcite crust. Arrow points to a gorgonin layer near the outer margin of the skeleton used as a chronological tie-in point. $\Delta^{14}\text{C}$ in this sample measured $-27 \pm 4 \text{ ‰}$; based on calibration to the local bomb- ^{14}C curve (Fig. 3C) it was formed in the year 1961 ± 5 . White lines indicate sub-samples for ^{210}Pb analysis. (B) ^{210}Pb data for specimen COHPS2001-1. Solid curve is the solution to the ^{210}Pb decay equation at the indicated growth rate (GR). Error bands (dashed curves) and vertical bars are 1σ errors; horizontal bars represent widths of sub-samples. (C) ^{210}Pb data for *K. ornata* specimen 1343. This specimen was collected alive; therefore the date of collection (2006) was used as the tie-in point.



575
576

Fig. 3: Paired gorgonin (surface water) and calcite (intermediate water) age-corrected $\Delta^{14}\text{C}$ records. (A) Hudson Strait records generated from 3 growth ring-dated colonies of *P. resedaeformis* (1525-1, 1525-3, 1525-10; depth = 414 m). (B) Southwest Grand Banks records generated from a single ^{210}Pb -dated *K. ornata* (1343; depth = 713 m). (C) Northeast Channel records from specimens of *P. resedaeformis* collected between 250-475 m. Gorgonin record from Sherwood et al. (2005); calcite record from the massive calcite zone of an older ^{210}Pb -dated colony (COHPS2001-1). Seawater $\Delta^{14}\text{C}$ data are from TTO and WOCE stations indicated in Fig. 1. 1σ errors in $\Delta^{14}\text{C}$ are smaller than symbols.

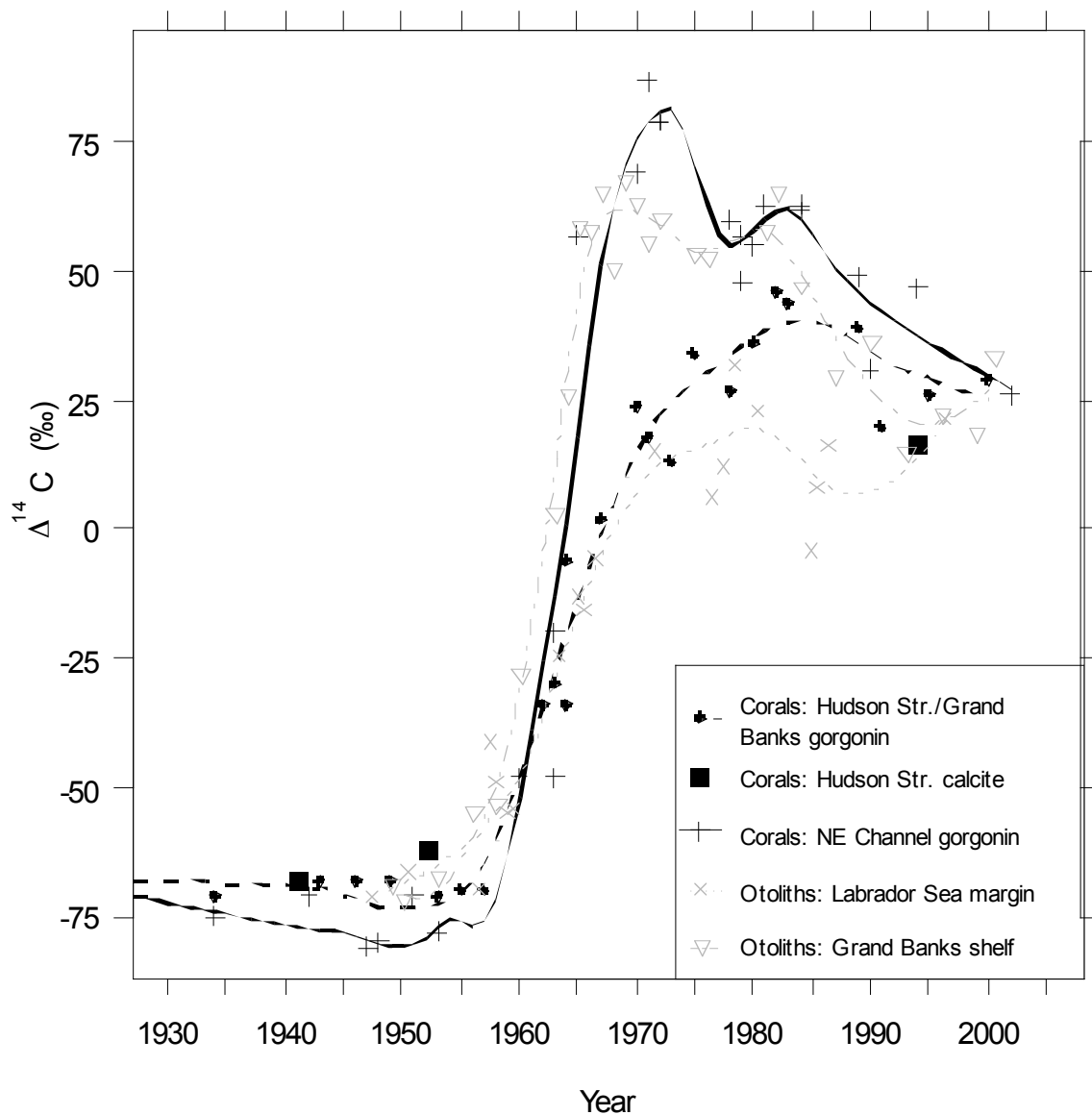


Fig. 4: Comparison of bomb- ^{14}C records from this study with those of Campana et al. (2008), derived from otoliths extracted from fish of age 0-3 years collected from the northern and western margins of the Labrador Sea and the Grand Banks shelf.

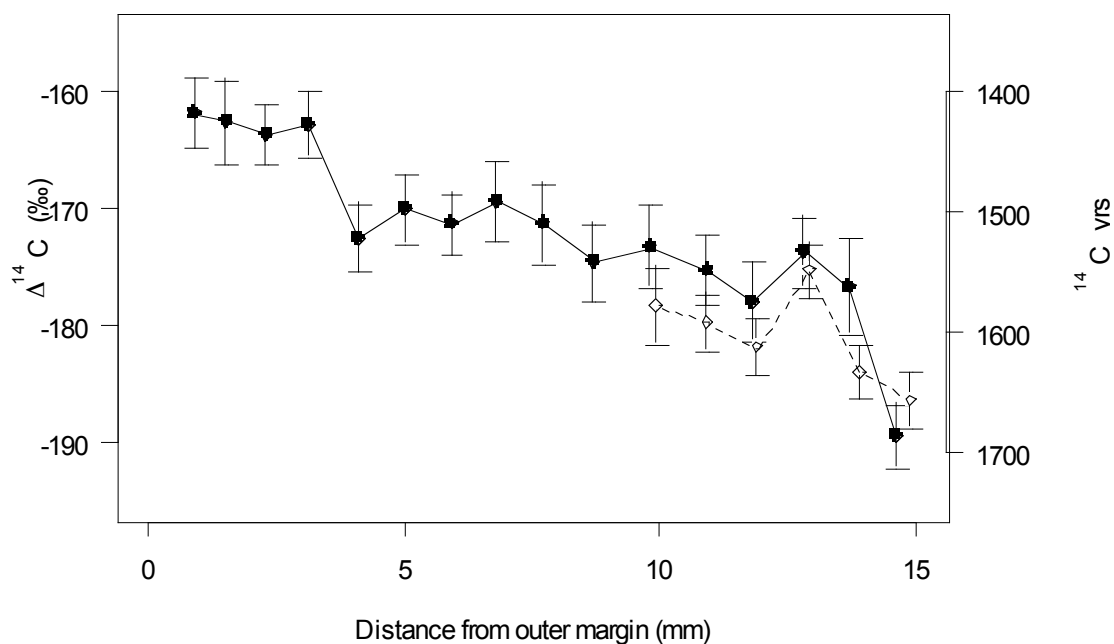


Fig 5: Radiocarbon data from a subfossil *K. ornata* (specimen 1449). Left-hand y-axis shows $\Delta^{14}\text{C}$; right hand y-axis shows corresponding ^{14}C age (uncalibrated). Paired gorgonin and calcite profiles were generated from the inner 5 mm of the sample; outer 10 mm was overgrown with calcite and gorgonin could not be sampled. Gorgonin and calcite profiles yield the same growth rate of 0.076 mm/yr, yielding a lifespan of 200 yrs.

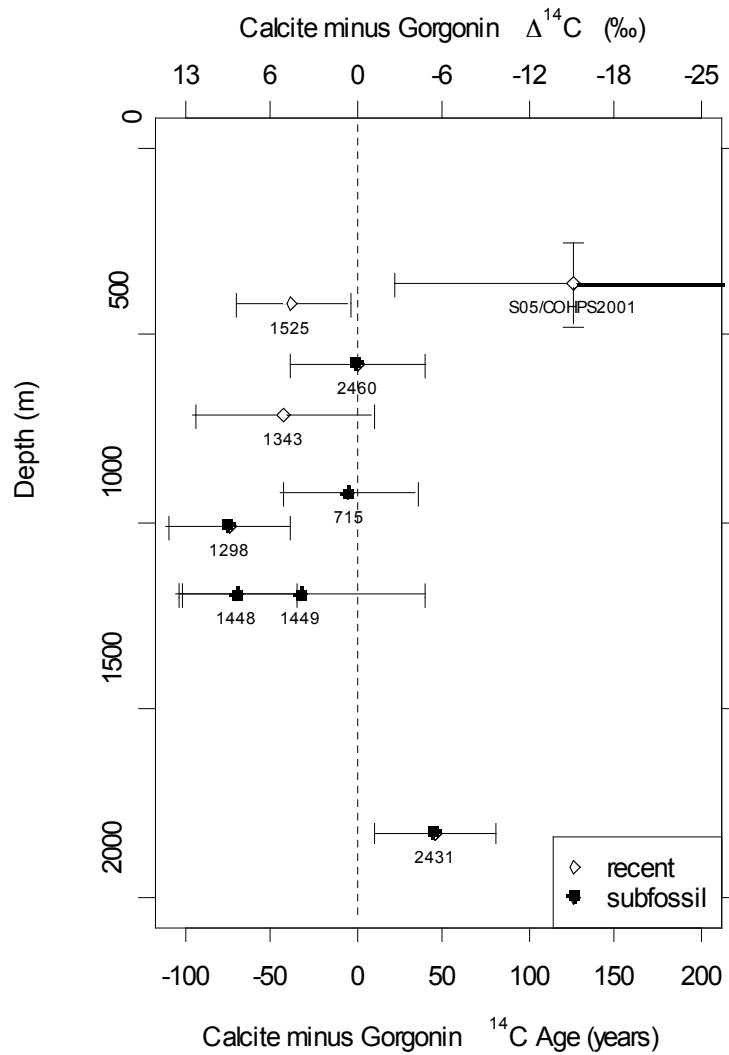


Fig. 6: Seawater vertical ^{14}C gradients derived from coeval samples of calcite and gorgonin from recent and subfossil corals. Sample codes correspond with those in Table 2. The line at zero represents a well mixed column of water. Positive values of the calcite minus gorgonin ^{14}C age represent a normally stratified water column with younger waters overlying older waters (e.g. samples 2431 (Sable Gully) and S05/COHPS2001 (Northeast Channel). Reverse stratification is indicated by the remaining samples, all of which were collected northward of the Scotian Slope. Corresponding calcite minus gorgonin $\Delta^{14}\text{C}$ is indicated along the upper x-axis. Errors are 1σ .